

University of Nebraska - Lincoln

DigitalCommons@University of Nebraska - Lincoln

Anthony F. Starace Publications

Research Papers in Physics and Astronomy

November 2000

Control of Intense Laser- Atom Processes With Strong Static Fields

Dejan B. Milosevic

University of Nebraska - Lincoln

Anthony F. Starace

University of Nebraska-Lincoln, astarace1@unl.edu

Follow this and additional works at: <https://digitalcommons.unl.edu/physicsstarace>



Part of the [Physics Commons](#)

Milosevic, Dejan B. and Starace, Anthony F., "Control of Intense Laser- Atom Processes With Strong Static Fields" (2000). *Anthony F. Starace Publications*. 91.

<https://digitalcommons.unl.edu/physicsstarace/91>

This Article is brought to you for free and open access by the Research Papers in Physics and Astronomy at DigitalCommons@University of Nebraska - Lincoln. It has been accepted for inclusion in Anthony F. Starace Publications by an authorized administrator of DigitalCommons@University of Nebraska - Lincoln.

Control of Intense Laser-Atom Processes With Strong Static Fields

Dejan B. Milošević¹ and Anthony F. Starace

*Department of Physics and Astronomy, The University of Nebraska,
Lincoln, NE 68588-0111, U.S.A.*

Abstract. We analyze the use of strong static electric and magnetic fields for controlling two intense laser-atom processes: laser-assisted x-ray-atom scattering and high-order harmonic generation. We find that x-rays scattered from atoms in the presence of both a strong laser field and a strong static electric field can be boosted in energy many-fold by absorption of energy from the laser field. The spectrum of scattered x-ray intensity vs. the number of laser photons absorbed exhibits a rich plateau structure, whose key features may be understood using a classical analysis. We find also that the intensities of high-order harmonics can be increased by orders of magnitude in the presence of strong static magnetic or parallel electric and magnetic fields and also that the static electric field can introduce additional plateaus and cutoffs. The maximum values of the harmonic intensity correspond to values of magnetic field for which the return time of the ionized electron wave packet to the atomic core under the influence of the laser field (and the static electric field, if present) is an integer multiple of the classical cyclotron period.

INTRODUCTION

Atomic processes in the presence of intense fields continue to attract a great deal of attention [1–3]. Key goals of research in this area are to increase the intensities and frequencies of coherent light produced in these processes. In two recent works [4,5] we have demonstrated theoretically the possibility of controlling intense laser-atom interaction processes by employing strong, but experimentally feasible, static electric or magnetic fields. Thus, in Ref. [4] we demonstrated how a strong static electric field may induce a high-energy plateau for scattered x-ray photons in laser-assisted, x-ray-atom scattering in which the incident x-rays were assumed to have an energy of 50 eV. The scattered x-rays were shown to have energies up to well over 200 eV, making such a process an attractive one for realizing coherent x-rays in the “water window” [between the K shell absorption

¹) Present address: Max-Born Institut, Max-Born-Strasse, 2a, 12489 Berlin, Germany. On leave from Faculty of Science and Mathematics, Department of Physics, University of Sarajevo, Zmaja od Bosne 35, 71000 Sarajevo, Bosnia and Herzegovina.

edges of C (284 eV) and O (532 eV)], which would have important applications to imaging living biological structures by means of x-ray holography [6]. In Ref. [5], we demonstrated control of high-harmonic generation (HHG) by a linearly polarized laser field using a uniform static magnetic field parallel to the laser polarization. We predicted that particular values of the magnetic field can increase harmonic intensities by orders of magnitude. Our classical orbit calculations showed that these magnetic-field-induced intensity revivals occur when the return time for laser-driven motion of the electron back to the origin is a multiple of the cyclotron period for motion perpendicular to the laser polarization direction. We present here further results [7–9] on using strong electric and magnetic fields to control these two intense laser-atom processes.

The so-called “two-” and “three-step” physical models [10–12], which have been extremely useful for interpreting the above-threshold ionization (ATI) and high-order harmonic generation (HHG) processes, also prove reliable in interpreting intense laser-atom processes in the presence of strong static fields. We thus summarize these models briefly. The “first step” is the ionization of an atomic electron, while the “second step” is the propagation of a free electron in the laser field. Some of the characteristics of ATI can be explained using only these two steps. The “third step” is the collision between the electron, driven back by the laser field, and the atomic core, whereupon the electron can recombine with the ion, emitting a harmonic photon. This three-step model explains both the appearance of the plateau in the HHG process and the maximum energy of the harmonics at the cutoff, $n_{\max}\omega = I_0 + 3.17U_p$, where I_0 is the atomic ionization potential, $U_p = E_L^2/(4\omega^2)$ is the ponderomotive potential energy, and E_L and ω are the laser electric-field amplitude and frequency, respectively. (We use here atomic + SI units.) Alternatively, during the third step the electron can scatter from the atomic core, giving rise to rescattering effects in ATI. In this case, the third step can explain the appearance of the plateau in ATI with its cutoff at $10U_p$ [13]. The classical three-step model is consistent with results of quantum-mechanical calculations [14–20].

Although we use the 3-step physical model to interpret our results, all of our results are obtained from quantum-mechanical calculations, as described in detail elsewhere [4,5,7–9]. In brief, we solve the three-dimensional, time-dependent Schrödinger equation for an electron moving in the laser plus static field(s). The atom or negative ion target is represented by a zero-range potential or other model potential. The initial atomic or ionic state is assumed to be unaffected by the fields. A key approximation in both our own work [4,5,7–9] and that of others [14–20] is the so-called strong-field approximation (SFA), in which the Green’s propagator of the total system is replaced in intermediate states by the Volkov Green’s propagator, i.e., the influence of the atomic potential on the electron is neglected in comparison with that of the laser field (and the static external fields if present). The SFA fails [21] if the number of photons exchanged with the laser field is small: for ATI this corresponds to photoelectrons with energies close to the threshold, while for HHG it corresponds to low-order harmonics. (For a comparison of results using the SFA with those obtained by solving the time-dependent,

three-dimensional Schrödinger equation, see [21].) Analysis of intense laser-atom processes (i.e., ATI, HHG, and laser-assisted x-ray-atom scattering) starting from the appropriate quantum-mechanical amplitudes, applying the SFA, and evaluating the resulting amplitudes in a quasiclassical (stationary phase) approximation provides a more rigorous confirmation of the three-step model than does a purely classical calculation.

Note finally that the static fields in our calculations are much stronger than is typical of such fields in the laboratory. We emphasize, however, that the values of the fields employed in our calculations are of the same order of magnitude as those which have been achieved experimentally. For static electric fields, up to 3.5 MV/cm has been obtained in the rest frame of a fast atom or ion passing through a modest-valued static magnetic field in the laboratory [22]. The maximum reproducible laboratory magnetic fields which have been reported have an induction $B \approx 1000$ T [23]. In the experiment presented in Ref. [23] the useful volume having this maximum magnetic field consists of a cylinder approximately 1 cm in diameter and 10 cm long. The duration of such strong magnetic pulses is a few μs , which is much larger than the laser field pulse duration, so that we can consider the magnetic field as constant.

CONTROL OF PLATEAU STRUCTURES IN LASER-ASSISTED X-RAY—ATOM SCATTERING

Milošević and Ehlötzky [24] considered the effect of a laser field on x-ray-atom scattering, i.e.,

$$\gamma + A \longrightarrow A + \gamma', \quad (1)$$

where γ is the incident x-ray, having $\hbar\omega_\gamma = 50$ eV, A is the target atom (chosen to be the H atom), and, γ' is the scattered x-ray, having energy

$$\hbar\omega_{\gamma'} = \hbar\omega_\gamma + n\hbar\omega, \quad (2)$$

where n is a positive or negative integer, and ω is the frequency of the laser field. They found plateaulike structures in the differential cross section (DCS) as a function of the number of photons n exchanged with the laser field primarily for $n < 0$ (i.e., emitted photons), indicating scattered x-rays having lower energies. Milošević and Starace [4] showed that the addition of a static electric field gives rise to an extended plateau for $n > 0$ (i.e., absorbed photons), indicating scattered x-rays having substantially higher energies close to the “water window” energy region. Fig. 1 shows the forward direction DCS for laser-assisted x-ray-atom scattering in the two cases, with and without a strong static electric field, E_S . One sees that the static field does not affect either the intensity or the extent of the plateau for $n < 0$; however, for $n > 0$ the static field gives rise to a plateau extending up to $n \geq 160$, thereby boosting the scattered x-ray energies by nearly 200 eV.

As described in Ref. [4], these results may be interpreted by means of a classical analysis consistent with the three-step model. In brief, making use of the fact that the quantum-mechanical transition amplitude for absorption of the 50 eV incident photon followed by emission of the scattered x-ray is far more important than the one for the reverse order of events [24], we assume that an intermediate state electron is “born” at the origin with an initial kinetic energy $p_0^2/2 = \hbar\omega_\gamma - I_0$ at $t = t_0$. We then solve Newton’s equations for motion of this electron under the influence of the laser electric field and any static field also present. For all trajectories which return to the origin at time $t = t_0 + \tau$, i.e., $\mathbf{r}(t_0 + \tau) = 0$, we find the maximum of the kinetic energy of the returning electron as a function of the initial time t_0 . We then assume that the difference between the kinetic energies of the electron at the origin between t_0 and $t_0 + \tau$ is available to boost the scattered x-ray’s energy above that of the incident x-ray. In this way we are able to predict from these classical considerations the $n > 0$ cutoff at $n \approx 166$ [4]. These considerations also explain why no $n > 0$ plateau appears for $E_S = 0$: the intermediate state electron, following absorption of a 50 eV x-ray photon, has too much kinetic energy to be returned to the origin by the laser field alone. Addition of the static field not only reflects the intermediate state electron wave packet back to the origin, but also accelerates the electron to higher kinetic energies. In addition, if the electronic wave packet returns to the origin sooner, spreading of the wave packet is reduced, thereby increasing the intensity of the emitted (scattered) x-ray.

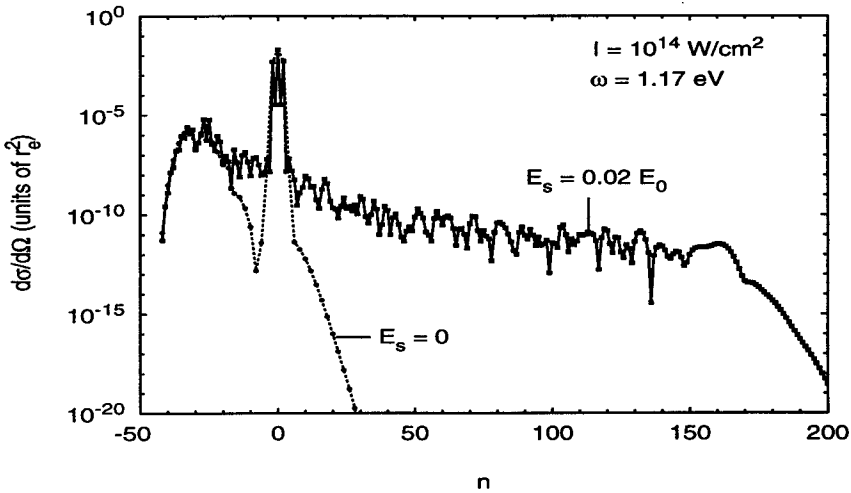


FIGURE 1. The DCS for x-ray–hydrogen atom scattering in units of r_e^2 (where $r_e = 2.8 \times 10^{-15}$ m is the classical electron radius) as a function of the number of photons n exchanged with the linearly polarized laser field of frequency $\omega = 1.17$ eV and intensity 10^{14} W/cm² (dashed curve). The results including a static electric field $E_S = 0.02E_0$ are shown by a solid line. ω_γ for the incident x-ray photons is 50 eV. (From Ref. [4].)

The classical interpretation of the results in Fig. 1 implies that the $n > 0$ plateau should be very sensitive to the value of the laser field intensity. Fig. 2 shows our results for five different laser field intensities, $I = i \times 10^{14}$ W/cm², $1 \leq i \leq 5$. A plateau for positive values of n appears as I increases, and, for the highest intensity, it is more than two times longer in n than the plateau for negative values of n , which remains almost unchanged for $I \geq 2 \times 10^{14}$ W/cm². For positive values of n , the energy of the scattered x-rays is increased and the shape of the plateau vs. n is very similar to that for a plot of HHG intensities, presented as a function of harmonic order [14,15,18,21]. For the HHG process, the cutoff of the plateau appears (for $U_p \gg I_0$) at $n_{\max}\omega \approx 3.17U_p$, where n_{\max} is the harmonic order. Figure 3 shows that this cutoff law is also valid for the laser-assisted x-ray-atom-scattering process. Namely, we present there $n_{\max}\omega$ in units of U_p as a function of the laser field intensity I , where now n_{\max} is the number of absorbed laser photons. For large values of I , i.e., for large values of U_p , we observe that $n_{\max}\omega \rightarrow 3.17U_p$ just as in the HHG process. A quasiclassical analysis (see Eq. (4) in Ref. [4]) shows that the proper cutoff law is $n_{\max}\omega = E_{k,\max} - \omega_\gamma + I_0$, where the maximum kinetic energy that the electron can acquire in the laser field is $E_{k,\max} = 3.17U_p$. For HHG, the cutoff formula for $n_{\max}\omega$ does not include a term $-\omega_\gamma$ because there are no x-ray photons in the initial state. Fig. 3 thus shows a clear connection between HHG and laser-assisted x-ray-atom scattering.

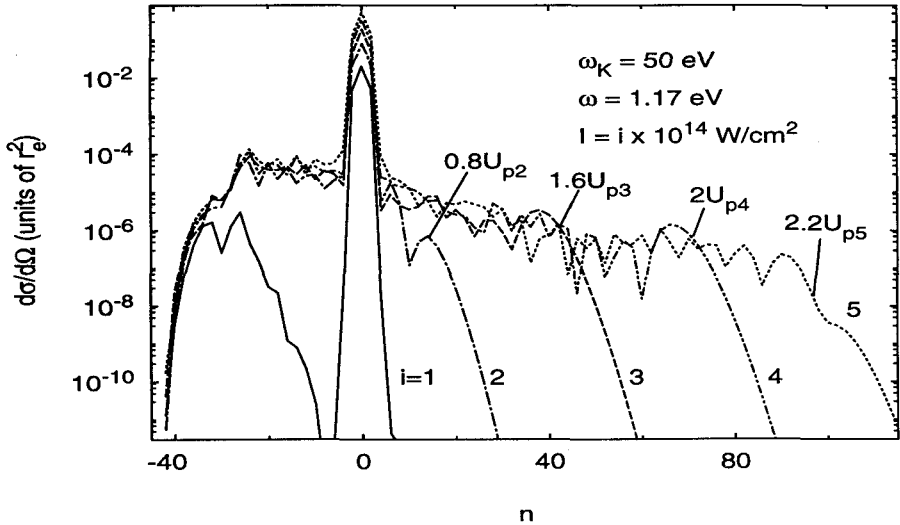


FIGURE 2. The same as Fig. 1 for $E_S = 0$ and for different laser field intensities $I(i) = i \times 10^{14}$ W/cm², where $i = 1$ (solid curve), 2 (dot-dashed curve), 3 (dashed curve), 4 (double-dot-dashed curve), and 5 (dotted curve). The energy cutoff positions are denoted by multiples of the ponderomotive potential energy U_{pi} for laser intensity $I(i)$. (From Ref. [7].)

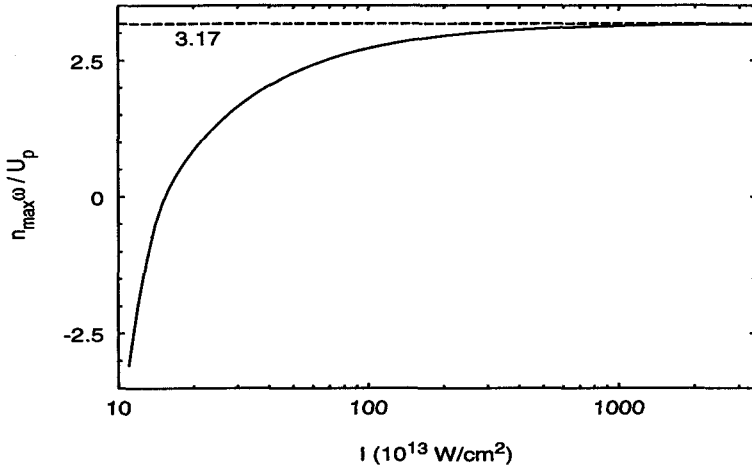


FIGURE 3. Maximum energy exchanged with the laser field in laser-assisted x-ray hydrogen-atom scattering, in units of the ponderomotive energy, as a function of the laser field intensity. The dashed line shows the $3.17 U_p$ cutoff of the HHG spectrum. The other parameters are as in Fig. 1, with $E_S = 0$. (From Ref. [7].)

In the presence of a static field $E_S = 2$ MV/cm, a very rich plateau structure appears as the laser intensity is varied [7]. This is similar to the multiple plateaus found for HHG in the presence of a static electric field [25]. For example, for a laser intensity $I = 5 \times 10^{14}$ W/cm², our calculations predict a (high intensity) plateau with a cutoff of $n = 100$, followed by a second (low intensity) plateau with a cutoff of $n = 569$. Each of these two cutoffs for each value of laser intensity I can be understood using a classical analysis, as detailed in Refs. [7,9].

MAGNETIC-FIELD-INDUCED INTENSITY REVIVALS IN HIGH-ORDER HARMONIC GENERATION

The three-step model of HHG implies that spreading of the intermediate state electronic wave packet reduces the probability of the electron's recombination with the atom or ion, thereby reducing the intensity of any harmonics emitted. Zuo *et al.* [26] proposed the use of a strong magnetic field to confine this spreading and demonstrated, for a two-color calculation, modest enhancement of HHG intensities for only one value of the magnetic induction, $B = 0.2B_0 = 47000$ T, where $B_0 = \hbar/(ea_0^2) = 2.3505 \times 10^5$ T. This value of B is much larger than the maximum presently achievable laboratory magnetic field [23]. Connerade and Keitel [27] also considered theoretically HHG in a strong magnetic field for the case of an intense pump laser. They focused on the possibility of generating even harmonics owing to relativistic motion of the laser-driven electron in the static magnetic field. Our

own interest in HHG in the presence of a strong static B field oriented parallel to the linearly-polarized laser field stems from the fact that there are two time scales involved for the motion of the intermediate state electron: the usual motion up and down the laser field polarization axis under the influence of the laser electric field, and, also, a periodic motion perpendicular to this direction with a period, τ_B , governed by the magnetic field, i.e.,

$$\tau_B = 2\pi/\omega_B = 2\pi/B, \tag{3}$$

where ω_B is the cyclotron frequency. We expected that when the time, τ , for the intermediate state electronic wave packet to return to the origin is an integer multiple of the cyclotron period, τ_B , then one might be able to increase the intensities of the harmonics generated.

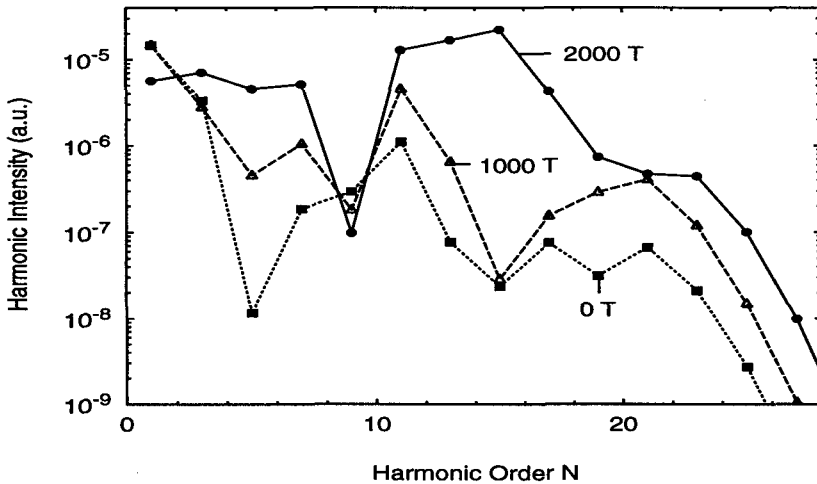


FIGURE 4. Harmonic intensities as functions of the harmonic order N for the H^- ion in a CO_2 laser with intensity $I_L = 5 \times 10^{10} \text{ W/cm}^2$. The magnetic field induction is $B = 0 \text{ T}$ (squares), 1000 T (triangles), and 2000 T (circles). (From Ref. [5].)

A typical set of results [5,8] is shown in Fig. 4, in which one sees that for some harmonics there are orders of magnitude increases in intensity, while for others the changes are modest. Figure 5 shows more clearly for the odd-order harmonics from 11 to 23 how their intensity varies as a function of the magnetic induction B . Clearly, for particular values of B there is a resonant-like increase in harmonic intensity for particular harmonics, which we call an “intensity revival.” The cause of these intensity revivals is indicated by a classical orbit analysis for the intermediate state electron [5,8,9]. Specifically, for a given harmonic we have calculated the period τ_i for the electron to be driven (along the z -axis) away from and then back to the origin for the i th time, and then compared these periods to the cyclotron

period, τ_B , for electronic motion perpendicular to the z -axis. These calculations show [5,8,9] that for the 15th and 17th harmonics in Figs. 4 and 5, $\tau_1 = \tau_B$, while for the 13th harmonic, $\tau_2 = 3\tau_B$. Also, for the 17th harmonic there is another revival for $\tau_1 = 3\tau_B$ (for a different value of B).

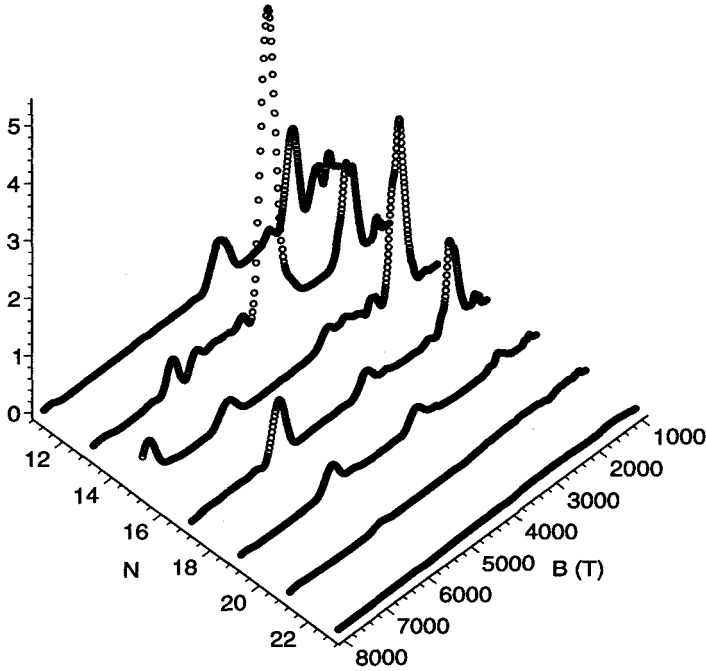


FIGURE 5. Harmonic intensities (in units of 10^{-5} a.u.) as functions of the harmonic order N and the magnetic field induction B . The laser field and the H^- ion parameters are as in Fig. 4. (From Ref. [8].)

In the presence of parallel B and E static fields, the HHG spectrum exhibits additional plateaus and cutoffs; also, the static electric field breaks the symmetry so that one observes both even and odd harmonics. Figure 6 shows our results [8]. As compared with the HHG spectrum in the absence of the static E field (cf. Fig. 4), one sees that the spectrum is extended to higher harmonics, with two additional cutoffs, at the 31st and the 43rd harmonics. Each of these cutoffs can be understood on the basis of a classical analysis [8]. One sees also that intensities of particular harmonics increase by two orders of magnitude as the magnetic field is increased from 1 to 3000 T. For any particular harmonic, its intensity variation as a function of magnetic field strength B can be understood in terms of a classical analysis [8,9].

We note finally that similar predictions for magnetic-field-induced revivals have been given for photodetachment of H^- in parallel E and B fields using both short

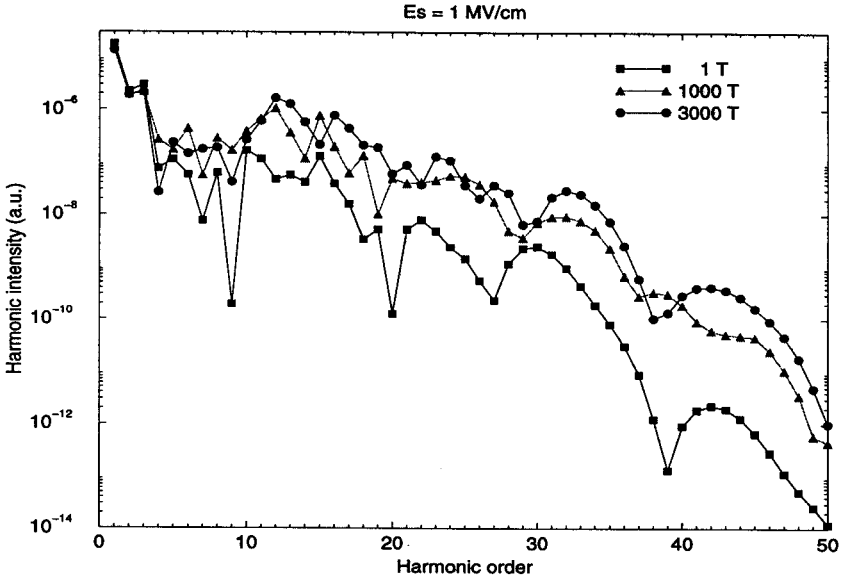


FIGURE 6. The same as in Fig. 4, but in the presence of a parallel static electric field having strength $E_S = 1$ MV/cm, for three values of the magnetic field induction: $B = 1$ T (squares), 1000 T (triangles), and 3000 T (circles). (From Ref. [8].)

and long pulse lasers [28]. In that case, it is the static electric field E which reflects photodetached electron wave packets back toward the H atom and the focus is on the final, photodetached state. In the present case, these electron motions occur in the intermediate state and their influence is reflected by the intensities of the generated harmonics.

CONCLUSIONS

We have shown how strong static electric and/or magnetic fields may be used to increase the intensities and/or energies of photons emitted in an intense laser-atom interaction process. Two such processes were considered: laser-assisted, x-ray-atom scattering and high-order harmonic generation. In each case our quantum mechanical predictions were interpreted by means of a classical analysis of the motion of the active, intermediate state electron. We note that the results we have shown do not by any means exhaust the possibilities for using strong static fields to control intense laser-atom interactions. In particular, we note work presented elsewhere at this conference concerning the use of a strong static electric field to control the polarization properties of the emitted harmonics in HHG [29].

ACKNOWLEDGMENTS

This work was supported in part by the U.S. National Science Foundation under Grant No. PHY-9722110. D.B.M. thanks the Alexander von Humboldt Foundation for research fellowship support.

REFERENCES

1. DiMauro, L. F., and Agostini, P., *Adv. At. Mol. Opt. Phys.* **35**, 79 (1995).
2. Protopapas, M., Keitel, C. H., and Knight, P. L., *Rep. Prog. Phys.* **60**, 389 (1997).
3. Salières, P., L'Huillier, A., Antoine, Ph., and Lewenstein, M., *Adv. At. Mol. Opt. Phys.* **41**, 83 (1999).
4. Milošević, D. B., and Starace, A. F., *Phys. Rev. Lett.* **81**, 5097 (1998).
5. Milošević, D. B., and Starace, A. F., *Phys. Rev. Lett.* **82**, 2653 (1999).
6. Spielmann, C., *et al.*, *Science* **278**, 661 (1997).
7. Milošević, D. B., and Starace, A. F., *Phys. Rev. A* **60**, 3943 (1999).
8. Milošević, D. B., and Starace, A. F., *Phys. Rev. A* **60**, 3160 (1999).
9. Milošević, D. B., and Starace, A. F., *Laser Phys.* **10**, 1 (2000).
10. Kuchiev, M. Yu., *Pis'ma Zh. Eksp. Teor. Fiz.* **45**, 319 (1987) [*JETP Lett.* **45**, 404 (1987)].
11. Kulander, K. C., Schafer, K. J., and Krause, J. L., in *Super-Intense Laser-Atom Physics*, ed. B. Piraux, A. L'Huillier, and K. Rzażewski, NATO Advanced Science Institutes Series, Series B: Physics Vol. 316 (Plenum, NY, 1993), p. 95.
12. Corkum, P. B., *Phys. Rev. Lett.* **71**, 1994 (1993).
13. Paulus, G. G., Becker, W., Nicklich, W., and Walther, H., *J. Phys. B* **27**, L703 (1994).
14. L'Huillier, A., Lewenstein, M., Salières, P., Balcou, Ph., Ivanov, M. Yu., Larsson, J., and Wahlström, C. G., *Phys. Rev. A* **48**, R3433 (1993).
15. Lewenstein, M., Balcou, Ph., Ivanov, M. Yu., L'Huillier, A., and Corkum, P. B., *Phys. Rev. A* **49**, 2117 (1994).
16. Becker, W., Lohr, A., and Kleber, M., *Quantum Semiclass. Opt.* **7**, 423 (1995).
17. Lewenstein, M., Kulander, K. C., Schafer, K. J., and Bucksbaum, P. H., *Phys. Rev. A* **51**, 1495 (1995).
18. Milošević, D. B., and Piraux, B., *Phys. Rev. A* **54**, 1522 (1996).
19. Lohr, A., Kleber, M., Kopold, R., and Becker, W., *Phys. Rev. A* **55**, R4003 (1997).
20. Milošević, D. B., and Ehlotzky, F., *Phys. Rev. A* **57**, 5002 (1998); **58**, 3124 (1998).
21. Antoine, Ph., Piraux, B., Milošević, D. B., and Gajda, M., *Laser Phys.* **7**, 594 (1997).
22. Bergeman, T., *et al.*, *Phys. Rev. Lett.* **53**, 775 (1984); Smith, W. W., *et al.*, in *Atomic Excitation and Recombination in External Fields*, edited by M. H. Nayfeh and C. W. Clark (Yordon and Breach, New York, 1985), p. 211.
23. Kudasov, Yu. B., *et al.*, *Pis'ma Zh. Eksp. Teor. Fiz.* **68**, 326 (1998) [*JETP Lett.* **68**, 350 (1998)].
24. Milošević, D. B., and Ehlotzky, F., *Phys. Rev. A* **58**, 2319 (1998).
25. Lohr, A., Becker, W., and Kleber, M., *Laser Phys.* **7**, 615 (1997).

26. Zuo, T., Bandrauk, A. D., Ivanov, M., and Corkum, P. B., *Phys. Rev. A* **51**, 3991 (1995); Zuo, T., and Bandrauk, A. D., *J. Nonlinear Opt. Phys. Mater.* **4**, 533 (1995); Bandrauk, A. D., *et al.*, *Int. J. Quantum Chem.* **64**, 613 (1997).
27. Connerade, J. -P., and Keitel, C. H., *Phys. Rev. A* **53**, 2748 (1996).
28. Wang, Q., and Starace, A. F., *Phys. Rev. A* **51**, 1260 (1995); **55**, 815 (1997).
29. Borca, B., Flegel, A. V., Prolov, M. V., Manakov, N. L., Milošević, D. B., and Starace, A. F., "Static-Electric-Field-Induced Elliptic Dichroism and Polarization Control of HHG," Abstracts of the 8th International Conference on Multiphoton Processes, Monterey, CA, 3-8 October 1999, Abstract No. IX.